# Residual Helmet Deformation from Non-Penetrating Ballistic Impacts on Various Head Surrogates

E. Butler[1], C. Howes[1], N. Hahne[1], Q. Luong[1], M. Clark[2], **A. Iwaskiw[1]**

*[1]The Johns Hopkins University Applied Physics Laboratory (JHU/APL), 11100 Johns Hopkins Road, Laurel, MD 20723, alexander.iwaskiw@jhuapl.edu*
*[2] U.S. Special Operations Command, 10 General Greene Avenue, Natick, MA 01760*

**Abstract.** Ballistic performance of helmets is affected by boundary conditions including the backing material (e.g., clay, air, skull) behind the helmet. This is a critical factor when developing and employing test methods and test equipment such as head surrogates. By comparing residual armour backface deformation (BFD) measurements from different backing-condition ballistic tests, the hope is to understand how particular helmet testing methods may influence helmet ballistic performance and material behaviour. This study assessed residual armour BFD measurements of helmets with different backing conditions: a clay headform, the Ballistic Load Sensing Headform (BLSH), the Adaptable Testing and Load Assessment System (ATLAS) Headform, and postmortem human surrogates (PMHS). PMHS were assumed to most accurately simulate the boundary conditions of live humans. Helmets were impacted with ballistic rounds at a range of velocities at four locations where the residual armour BFD was characterised. Results indicate comparable helmet BFDs between the PMHS-backed helmets and load cell headform-backed helmets. The clay-backed helmets had a larger range of peak residual BFDs, with the peak residual BFDs being nearly 15 mm greater than BFDs seen with PMHS-backed and load cell headform-backed helmets. Additionally, it was found that shot velocity was not a strong predictor of peak deformations across all backing types. This study demonstrates that backing materials and boundary conditions have an effect on helmet deformation behaviour and thus head surrogate materials and designs should be carefully considered. The measurements from this study are not meant to predict injury, but rather to understand the correlation between test conditions and the operational environment. These results indicate a potential need for test methodologies and test equipment to simulate the boundary conditions of armour in operational use as it will influence helmet performance during laboratory testing.

## 1. INTRODUCTION

Helmets play a crucial role in providing protection for the warfighter against a wide range of threats. Recent material advancements have led to the development of helmets capable of withstanding ballistic impacts from higher energy, small arms ammunition [1]. Modern helmets mitigate threats by dissipating kinetic energy and preventing armour perforation, thereby reducing the risk of penetrating ballistic injuries to the wearer [2]. Consequently, during impact the round causes rapid material deformation of the helmet. This deformation causes the backface of the helmet to strike the wearer potentially resulting in behind helmet blunt trauma (BHBT). BHBT can lead to severe injuries such as skull fracture, brain contusion, hematomas, and axonal injuries [3].

Given the critical need to protect warfighters, the ballistic performance criteria of helmets must be examined. This includes developing standardised measurement techniques to inform manufacturing processes. Ideally, a single test methodology would be used for both penetrating and non-penetrating ballistic performance assessments due to the cost associated with destructive testing. Previous studies have indicated that penetrating ballistic performance is influenced by backing material [4], [5]. This indicates the need for operationally relevant ballistic performance qualification testing including the use of biofidelic backing materials. While experiments to determine penetration levels associated with different backing materials are possible, they are costly and pose a risk of damaging expensive testing components such as load cells in headforms. An alternative approach is to analyse residual helmet backface deformation (Figure 1) to provide some insight into ballistic performance and allow for comparison across backing conditions [6].

https://doi.org/10.52202/081621-0054

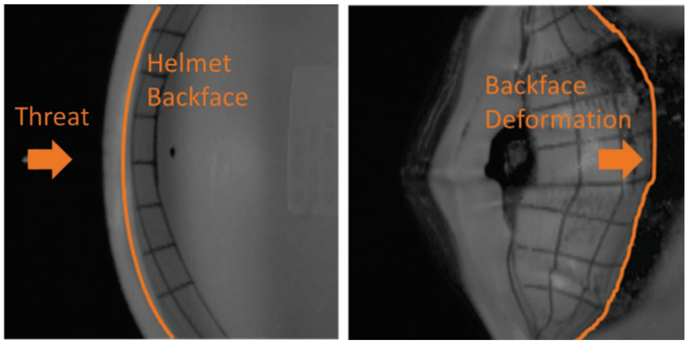

**Figure 1.** Undeformed helmet just prior to impact (left) with threat direction indicated and backface deformation of helmet during impact (right). Note the helmet used in this visual demonstration is not the helmet used in this study.

It is hypothesised that biofidelic test methods that simulate operational conditions are essential for obtaining representative ballistic performance measurements. Various platforms have been developed to evaluate helmet ballistic performance characteristics using different backing materials. Current ballistic performance measurements rely on a clay headform which provides a penetration outcome, and in cases where there is no complete penetration, a static measurement of the maximum deformation of a helmet in the impacted clay from a BHBT-induced event. However, clay testing does not capture dynamic load transfer during impact from BHBT. Surrogate headforms equipped with load cells were developed to understand this dynamic loading, but the effect these load cell backed headforms have on ballistic performance dynamics remains unclear. Additionally, ballistic performance testing has also been performed on postmortem human surrogates (PMHS) to understand BHBT related injuries, providing a realistic response comparable to the warfighter. Data collected across these backing conditions varies significantly which limits the ability to make direct comparisons of their effects on ballistic performance.

Residual BFD is defined as the backface deformation remaining in a deformed helmet after a non-penetrating ballistic impact. This residual deformation is typically less than the peak dynamic deformation of the backface due to the material rebound. Capturing maximum dynamic deformation is challenging due to the rate of the deformation and the obscured backface on a headform. Conversely, residual BFD measurements are taken after a ballistic event, allowing for the same collection technique to be used across backing conditions. This enables comparisons between experimental conditions to determine if the backing material affects the degree of helmet deformation during non-penetrating ballistic impact. If significant differences are observed, this suggests the need for helmet ballistic performance qualification testing to be performed on a backing material aligned with operational conditions to ensure accurate assessment of field performance. This study presents the residual backface deformation of a light weight helmet impacted with the same ballistic threat on various backing materials commonly used to assess helmet ballistic performance.

## 2. METHODS

### 2.1 General experimental methods

Each experimental set up utilised a modern lightweight helmet primarily composed of ultra-high molecular weight polyethylene that was fit to the head surrogate according to manufacturer instructions. Proper pads and suspension systems to achieve a 23mm±0.5 mm standoff[1] regardless of backing material were in place during testing. All ballistic testing was performed at an NIJ certified range (Element U.S. Space and Defense, Belcamp, Maryland, USA). The helmets were impacted with an 8.0 g (124 grain), 9 mm full metal jacket threat. The same armour-threat paring was used for each experimental setup. Velocities were varied to achieve a range of backface deformation without helmet penetration. The velocity range was chosen to align with previous PMHS tests where both injurious and non-injurious fracture outcomes were recorded. Projectile velocity measurements were obtained using infrared screen-based velocity gates (Oehler Research Model N0. 57) with universal counter chronographs (Hewlett-Packard model No. 53131A). Velocity was measured 1.5 m from the surface of the helmet, then velocity

---

[1] Airgap between backface of the helmet and underlying surface

loss equations were applied specific to the projectile to calculate striking velocity. The distance between the barrel and surface of the helmet was held consistent across test setups at 4.6 m. The crown, front, side, and rear impact locations (Figure 2) were chosen to remain consistent with current clay standard testing protocols used to define allowable clay deformation for helmets. The NVG mount was removed for all tests, while the ARC rails were left on but not directly impacted during the tests. All tests were conducted with the same 0° obliquity at each shot location where the ballistic striking vector was normal to the impact location.

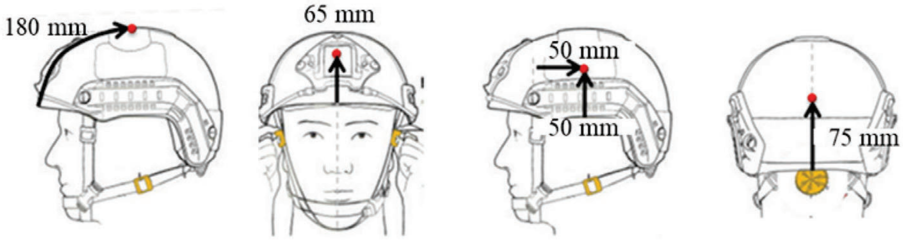

**Figure 2**. Helmet impact locations (red circle) for (left to right) crown, front, left side, and rear. Arrows indicate direction of measured distance across the surface of the helmet.

## 2.2 Experimental setup

In this study, four backing materials were characterised for their effects on residual backface deformation: the multi-sized clay headform, the Adaptable Testing and Load Assessment System (ATLAS) Headform, the Ballistic Load Sensing Headform (BLSH), and PMHS. This study collected ballistic impact velocity and residual BFD measurements for each of the four experimental conditions. Identical ballistic test methods were used across the four setups to allow for the comparison of each type of backing material.

### *2.2.1 Clay-headform backed experimental setup*

The clay backface deformation measurement is a key metric in helmet ballistic performance qualification [7]. In this standardised test protocol, the multi-sized clay headform (size Medium/Large) was packed and moulded with temperature-calibrated Roma Plastilina No. 1 clay and the helmet was fit as previously described. The external geometry of this headform was standardised to uniformly produce the 23 mm standoff distance for each impact location when outfitted with the tested helmet. The test range was controlled within test standards to an ambient temperature of 20ºC ±12ºC and 50 ±20% relative humidity. The headform was rigidly mounted on a fixture that allowed for vertical, horizontal, and rotational adjustments to achieve the desired obliquity.

The helmet was then impacted with a non-penetrating ballistic round. After testing, the helmet was removed and the maximum depth of the indented clay was measured to define the clay backface signature for a specific armour-threat pairing. As this is a widely accepted standard for helmet performance testing, impact locations, velocities, and general experimental set up for remaining residual BFD test protocols was modelled off the clay standard test protocol.

A total of 56 clay backed tests for this study were performed according to the standardised helmet ballistic performance qualification tests. Figure 3 shows the helmeted clay headform prior to ballistic impact (top row) and indented clay headform after the helmet was removed post-impact (bottom row).

https://doi.org/10.52202/081621-0054

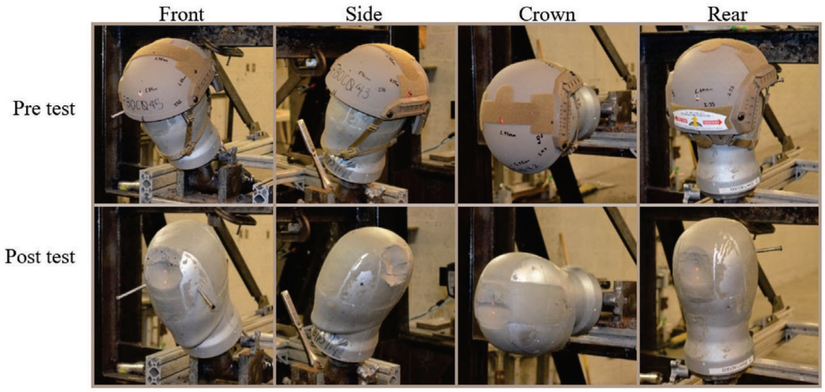

**Figure 3.** For each impact location, an intact helmet (top) fit onto the clay headform and the deformed headform (bottom) after a non-penetrating ballistic impact at the point indicated by the laser.

### *2.2.2 The Adaptable Testing and Load Assessment System (ATLAS) headform experimental setup*

The ATLAS headform (JHU/APL, Laurel, Maryland, USA) is a load-cell based surrogate headform developed to evaluate helmet performance and the potential for BHBT [8]. The system consists of modular headforms used to test each of the impact locations described in Table 1, where the centre of the load cell is positioned directly under the impact location. Figure 4 shows a schematic of the headform configured for a front impact test. The ATLAS headform is additively manufactured from acrylonitrile butadiene styrene (ABS-M30) and polyurethane elastomer (Huntsman RenCast 6443) and equipped with a stainless-steel impact cap (304/304L) with an outer radius that conformed to the curvature of the headform at each impact location. A neoprene impact pad with a thickness of 12.7 mm covered the impact cap and contoured with the headform. The impact cap was magnetically attached to a piezoelectric load cell (111 kN, 224C/FCS-DI IC, PCB Piezotronics) and attached to a post and base assembly. The headform base was then fixed to a ballistic alignment fixture. The ATLAS headform was used to collect non-penetrating ballistic impact data across four shot locations for a total of 45 shots.

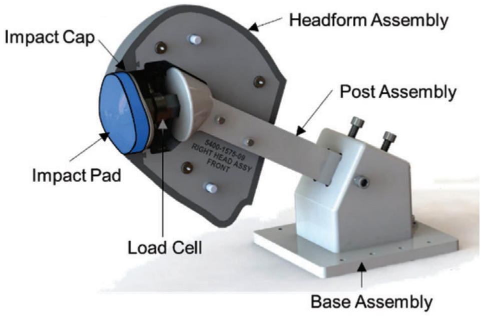

**Figure 4**. Schematic of ATLAS Headform system components. Schematic shown is for the front impact configuration.

### *2.2.3 The Ballistic Load Sensing Headform (BLSH) experimental setup*

The Ballistic Load Sensing Headform (BLSH) (Biokinetics and Associates Ltd., Ottawa, Canada) is used to assess BHBT from non-penetrating ballistic impacts [9]. The headform was mounted on a flexible neck and was equipped with an array of 7 load cells (Figure 5) at each impact location to measure contact force, distribution, and impulse during ballistic impact. A metal impact cap was mounted to each load cell, and a silicone rubber skin pad covered each array of 7 impact caps. The BLSH experimental setup was similar to that of the ATLAS Headform where the centre of the loadcell array was aligned with the intended impact location. A total of 7 non-penetrating shots were conducted.

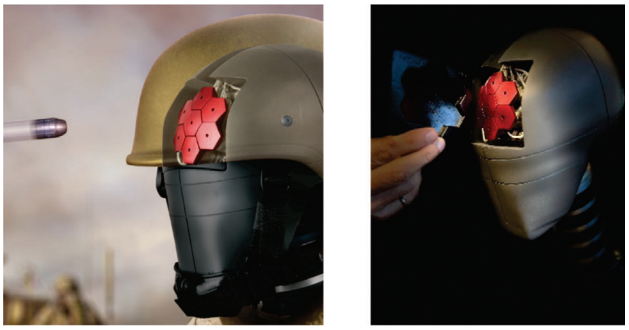

**Figure 5**. Biokinetics Ballistic Load Sensing Headform with transparent helmet to highlight use of front location - silicone skin pad not shown (left) and BLSH front impact location with impact pad held to side (right) [10].

### *2.2.4 Postmortem human surrogates (PMHS) experimental setup*

Experimental testing with PMHS offers insight into the biomechanical response to ballistic impacts warfighters may face, providing what is likely the most biofidelic backing condition. This study uses data collected by JHU/APL, detailed in Iwaskiw, et al. [11]. Exclusion criteria related to bone health, head size, and age were implemented to select fresh frozen specimens to reduce variability in the experiment. The specimens were affixed to a rigid suspension fixture to allow for alignment of target anatomy with the path of the projectile for all shot locations (Figure 6). A total of 58 non-penetrating shots were analysed for this study.

**Figure 6**. Approximate anatomical impact locations for the crown (red), front (green), left Side (blue), and rear (purple) for the PMHS experimental setup

### *2.2.5 Test matrix and experimental summary*

Table 1 summarises the four experimental conditions used for data collection in this study. It includes a breakdown of impacts at each location for all backing conditions.

**Table 1.** Summary of experimental setup for various backing materials.

| | **Clay-Headform** | **ATLAS** | **BLSH** | **PMHS** |
|---|---|---|---|---|
| Backing Material | Clay | Neoprene pad, metal impact cap, and load cell | Silicone pad, metal impact caps, and load cells | Skin/skull |
| Helmet | Modern lightweight ultra-high molecular weight polyethylene | | | |
| Standoff | 23 mm ± 0.5 mm | | | |
| Threat | 8.0 g (124 grain), 9 mm full metal jacket | | | |
| Velocity Range (m/s) | ~280 – ~450 | | | |
| Distance to barrel (m) | 4.6 | | | |
| Obliquity | Held consistent across experimental setups | | | |
| Crown Impacts | 13 | 10 | 0 | 11 |
| Front Impacts | 18 | 12 | 1 | 16 |
| Side Impacts | 12 | 8 | 6 | 16 |
| Rear Impacts | 13 | 15 | 0 | 13 |
| Total Impacts | 56 | 45 | 7 | 58 |

### 2.3 Residual BFD measurement technique

Residual BFD is measured by comparing the surface scan of an intact helmet to the surface scan of a tested helmet (Figure 1). A coordinate measurement machine (ROMER Absolute Arm, 7535SEI-3401-UC, Hexagon Manufacturing Intelligence, North Kingstown, RI) was used to scan each helmet's backface surface post-test, creating a point cloud representation of the residual BFD. The intact helmet was also scanned for a reference surface. All helmets were scanned using a standard fixture to assist with co-registration in 3D space. Metrological inspection software (Geomagic Control X, 3D Systems, Rock Hill, South Carolina, USA) was used to process the data scans to generate a digitised version of each helmet surface. A tested helmet scan and the intact helmet scan were loaded into the software and coregistered. The deviation analysis method used involved comparing the measured data from a tested helmet to the intact helmet surface by calculating the shortest distance between paired points. The measured points are projected onto the reference data using the shortest distance calculation.[2] This method generates a colour deviation map, visually representing positive and negative deviations across the entire part seen in Figure 7.

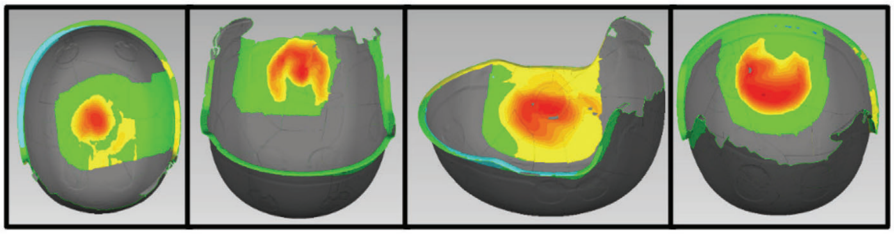

**Figure 7.** Point clouds scans of shot helmets at (left to right) crown, front, side, and rear impact locations. Each helmet is oriented to have a straight on view of the deformation surface (i.e. inside surface). Colour map (scale not shown) represents varying levels of deformation from the intact surface (grey). Light blue/green indicates minimal deformation, orange/red indicates maximum deformation

## 3. RESULTS

Maximum residual BFD was recorded with respect to impact velocity for each of the helmets tested (Figure 8). The range of residual BFD results across all backing conditions was 5.88 mm to 39.56 mm. The crown impact location consistently had the lowest residual BFD measurements, regardless of backing material (Figure 9). The front impact location had the highest residual BFD for all but the PMHS backing condition. In clay and ATLAS backed tests, deformation was highest at the front impact location, followed by rear, average over all locations, side, then crown (Figure 9). Although deformation magnitude varied by backing condition, this trend of differences in magnitude for a given backing condition across impact locations was a notable finding of the study. While the BLSH backed results were included in this study, there are significantly less impacts for this test condition. These results were included in the current study but were originally collected for a different purpose.

---

[2] This was executed through the "3D Compare/Shortest" method

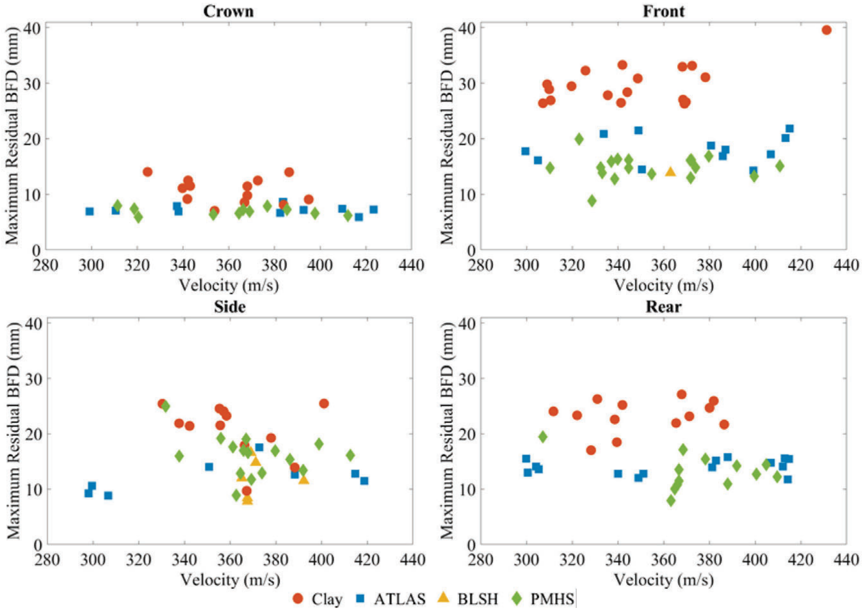

**Figure 8.** Point of maximum residual BFD results by impact location and backing condition.

Helmet tests on the clay headform resulted in the highest residual BFD measurements across all shot locations (Figure 9), while the three other backing materials had more similar residual BFDs. An initial single factor Analysis of Variance (ANOVA) was conducted to compare the means of residual BFD for all backing materials. The resulting p-value was 0.0000, indicating that at least one of the groups was significantly different from the others. In order to determine which groups were statistically different, a Tukey's honestly significant difference (HSD) test was conducted to do pairwise comparisons of each of the backing materials. Clay was statistically different from each of the other backing conditions with p-values less than 0.0001. The ATLAS Headform and BLSH were not statistically different with a p-value of 0.9640. The BLSH and PMHS were not statistically different with a p-value of 0.9601. The ATLAS Headform and PMHS were not statistically different with a p-value of 1.000. This initial analysis considered all shot locations in the groups. The full analysis results are in Table 2.

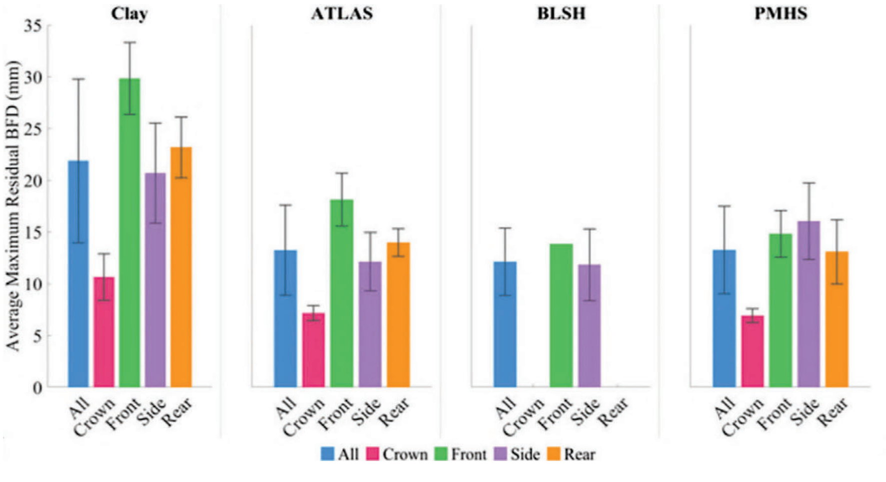

**Figure 9.** Average maximum residual BFD results by impact location and backing condition with standard deviations included

The same analysis process was conducted to compare the mean residual BFD for each backing condition across shot locations. For all impact locations, the clay residual BFD measurements were significantly different from all other backing materials. For the crown and rear impact locations, the ATLAS Headform and PMHS backing conditions were not significantly different. The BLSH was not considered for crown or rear impact location analysis. For the side impact location, the ATLAS Headform was not significantly different from the BLSH or the PMHS. The BLSH and PMHS were also not significantly different at this location. For the front impact location, the ATLAS Headform and the BLSH were not significantly different. The BLSH and PMHS were not significantly different. The ATLAS and PMHS were significantly different.

**Table 2**. Tukey's honestly significant difference (HSD) results for determining significant differences in mean residual BFD on various backing materials across shot locations. Residual BFD mean differences are significant at the 0.05 level. Groups with means that were statistically significant are indicated with (*).

| **Impact Location** | **Group 1** | **Group 2** | **Mean Difference (mm)** | **95% Confidence Interval** | **P-value** |
|---|---|---|---|---|---|
| All | Clay | ATLAS | 8.63 | (5.67, 11.6) | 0.0000 |
| | | BLSH | 9.74 | (3.82, 15.7) | 0.0001 |
| | | PMHS | 8.60 | (5.84, 11.4) | 0.0000 |
| | ATLAS | BLSH | 1.12 | (-4.89, 7.12) | 0.964* |
| | | PMHS | -0.02 | (-2.96, 2.91) | 1.000* |
| | BLSH | PMHS | -1.14 | (-7.05, 4.77) | 0.960* |
| Crown | Clay | ATLAS | 3.45 | (1.94, 5.04) | 0.000 |
| | | PMHS | 3.74 | (2.22, 5.25) | 0.000 |
| | ATLAS | PMHS | 0.25 | (-1.36, 1.86) | 0.924* |
| Front | Clay | ATLAS | 11.7 | (8.87, 14.5) | 0.000 |
| | | BLSH | 16.0 | (8.18, 23.8) | 0.000 |
| | | PMHS | 15.0 | (12.5, 17.5) | 0.000 |
| | ATLAS | BLSH | 4.28 | (-3.62, 122) | 0.478* |
| | | PMHS | 3.31 | (0.484, 6.14) | 0.0159 |
| | BLSH | PMHS | -0.969 | (-8.77, 6.83) | 0.987* |
| Side | Clay | ATLAS | 8.54 | (3.76, 13.3) | 0.0001 |
| | | BLSH | 8.84 | (3.60, 14.0) | 0.0003 |
| | | PMHS | 4.64 | (0.640, 8.64) | 0.0175 |
| | ATLAS | BLSH | 0.295 | (-5.36, 5.95) | 0.999* |
| | | PMHS | -3.90 | (-8.44, 0.631) | 0.113* |
| | BLSH | PMHS | -4.20 | (-9.21, 0.814) | 0.128* |
| Rear | Clay | ATLAS | 9.20 | (6.86, 11.5) | 0.000 |
| | | PMHS | 10.1 | (7.67, 12.5) | 0.000 |
| | BLSH | PMHS | 0.894 | (-1.45, 3.23) | 0.624* |

## 4. DISCUSSION

It is hypothesised that ballistic helmet performance is influenced by multiple factors and residual backface deformation could be an indicator of this performance. This gives insight into the helmet's ability to stop a round from penetrating and to prevent BHBT injuries from non-penetrating events. This post-test measurement reveals evidence of different deformation patterns for less biofidelic backing materials.

Regional variations in maximum residual BFD calls for additional exploration. The front impact location had the highest maximum residual BFD for all but the PMHS backing condition. This may indicate there are geometric effects caused by the unique interaction between the 3D curvature of the helmet and the backing material. This may be driving the differences when compared to PMHS. The front impact location also had HSD results that did not agree with trends for the other impact locations across backing conditions. Further analysis should be done to confirm these potential sources of region-specific residual deformation effects.

From Figure 9, the standard deviation for some backing conditions is higher when considering the total group compared to each individual impact location. This can be explained by the differences in mean residual BFD between impact locations. The PMHS mean residual BFD was 0.02 mm greater than the ATLAS Headform mean and 1.14 mm greater than the BLSH mean. The clay mean residual BFD was at least 8.60 mm greater than the other surrogate headforms. Considering the standard deviations reported, it is plausible the differences in mean of the PMHS, ATLAS, and BLSH could be within the noise of the measurement systems used to collect residual BFD.

The clay backing material was the only one that resulted in mean helmet deformations at various impact locations greater than the airgap reported earlier. This is evidence of a rebound phenomenon occurring for the load cell and PMHS backed conditions that is much less significant or not present in clay backed tests. This could highlight the role in the stiffness of the backing material to residual deformation, where the typical Young's modulus values in literature of steel (approximately 100-200 GPa) [12] and skull (18 GPa) [13] are larger than clay (150 MPa) [14].

Examining Figure 8, differences can be seen in residual BFD across backing materials, but there is no clear correlation between residual BFD and velocity across the velocity range tested. The expectation would be for a positive linear relationship, but this is not seen across any backing material. The reason for this non-intuitive trend is unclear. This study did not cover a wide range of ballistic velocities. A larger velocity range, especially at lower velocities, may reveal a more intuitive trend between velocity and residual BFD. One hypothesis for the observed behaviour is the stiffness of the backing material has a stronger influence on residual BFD than the threat at this higher range. A study using soft armour and a 9 mm threat saw that backing material stiffness had a significant impact on the deformation response [15]. Another hypothesis is that the volume of the residual backface deformation may have a stronger correlation to velocity than the peak deformation. A previous study found if the backing material is stiff enough, it could arrest deformation in the shot direction where transverse deformation (radial to the shot direction) is unconstrained by backing material stiffness [16]. Further analysis of the residual backface volume would be needed to confirm this hypothesis.

Multiple factors constrain this study and the analysis done on the results. Residual BFD was collected as a one-dimensional metric. Other techniques could have been used in place of this measurement such as volume, surface area, or BFD shape. The one-dimensional metric was chosen for consistency with the clay standard test metric for max deformation. The other metrics have not yet been fully explored for this study, however additional analysis of the results may be suitable for comparison with results of previous studies [16]. Lastly, this study explores the relationship between residual BFD and backing material for one armour-threat pairing, and it is unknown if these findings can be extended to other armour or threats.

## 5. CONCLUSION

The results of this study show that helmet backing condition affects at least one aspect of an armour performance correlate, residual helmet BFD, and thus it is important to consider helmet backing conditions when performing helmet ballistic testing. Of the four backing conditions evaluated in this study, it is assumed that PMHS best simulates the backing condition of a living individual. For the same range of input velocities, ballistic helmet testing on the clay headform resulted in significantly higher residual BFD measurements than helmets tested on PMHS, whereas helmets tested on the BLSH and ATLAS Headform had residual BFD results that closely aligned to results from PMHS, suggesting these load cell backed headforms are more biofidelic than clay platforms.

To ensure warfighter protection when helmets are fielded, helmets should be tested in a manner that sufficiently simulates the operational environment to accurately assess helmet performance. While the relationship between residual helmet deformation measurements and penetrating and non-penetrating ballistic response of the helmet remains to be determined, the results of this study indicate there could be differences in helmet performance that are not captured accurately when testing helmets on backing materials that are significantly different than PMHS.

## Acknowledgements

The authors would like to express their appreciation to the U.S. Special Operations Command for funding this work under Contract No. H92236-10-D-001, Task Order 0521.

https://doi.org/10.52202/081621-0054

## References

[1] Y. Li, H. Fan, X.-L. Gao, “Ballistic Helmets: Recent advances in materials, protection mechanisms, performance, and head injury mitigation,” *Compites Part B: Engineering ,* p. 109890, 2022.

[2] K. Loftis, E. Matheis and K. Rafaels, “Assessment of Head Injuries: Blunt versus Penetrating,” in *Proceedings of the Personal Armour Systems Symposium*, Cophenhagen, Denmark, 2020.

[3] V. Nair, et al., “Review of Department of Defense Test Protocols for Combat Helmets,” National Research Council, Washington DC, 2014.

[4] T.-T. Nguyen, et al., “The Critical Role of a Backing Material in Assessing the Performance of Soft Ballistic Protection,” *Journal of Transformative Technologies and Sustainable Development,* 2022.

[5] G. James, et al., “The effect of backing methods on the measure ballistic performance of armour materials,” Platform Systems Division, Wiltshire.

[6] M. Bevan, et al., “Effect of Backing Material on Residual Armor Deformation,” in *Proceedings of the Personal Armour Systems Symposium*, Copenhagen, Denmark, 2020.

[7] Y. Li, et al., “Review of mechanisms and research methods for blunt ballistic head injury,” *Journal of Biomechanical Engineering,* 2023.

[8] M. Trexler, et al., “Development of a Modular Load-Sensing Headform,” in *Personal Armour Systems Symposium*, Washington DC, 2018.

[9] M. Philippens, et al., “Results of a Round Robin Ballistic Load Sensing Headform,” in *Personal Armour Systems Symposium*, Cambridge, 2014.

[10] Biokinetics, “Ballistic Load Sensing Headform,” Biokinetics, 24 February 2025. [Online]. Available: https://biokinetics.com/prouct/ballistic-load-sensing-headform/. [Accessed 24 February 2025].

[11] A. Iwaskiw, et al., “Loads Assoicated with behind helmet blunt trauma: Matched-pair load sensing headform tests correlated with skull fracture severity,” in *Personal Armour Systems Symposium*, Dresden, 2023.

[12] Z. Chen, “Variation and consistency of Young’s modulus in steel,” *Journal of Materials Processing Technology,* vol. 227, pp. 227-243, 2016.

[13] A. D. Brown, “Shear behavior of human skull bones,” *Journal of Mechanical Behavior of Biomedical Materials,* vol. 116, p. 104343, 2021.

[14] E. Carton, “Characterization of dynamic properties of ballistic clay,” in *Personal Armour Systems Symposium*, Cambridge, 2014.

[15] T. Goode, “Soft body armor time-dependent back face deformation (BFD) with ballistics gel backing,” *Composite Structures,* vol. 220, pp. 687-698, 2019.

[16] Y. Zhu, “Ballistic impact wave and bulge profile propagation characteristics and blunt injury assessment of UHMWPE laminate composite,” *Journal of Materials Research and Technology,* vol. 31, pp. 3760-3780, 2024.

https://doi.org/10.52202/081621-0054